Statistical Properties of Electron Curtain Precipitation Derived with AeroCube-6

M. Shumko[1], A.T. Johnson[1], T.P. O'Brien[2], D.L. Turner[3], J.G. Sample[1], J.B. Blake[2], L.W. Blum[4], A.J. Halford[4]

[1]Department of Physics, Montana State University, Bozeman, Montana, USA
[2]Space Science Applications Laboratory, The Aerospace Corportation, El Segundo, California USA
[3]Johns Hopkins Applied Physics Laboratory, Laurel, Maryland, USA
[4]NASA's Goddard Space Flight Center, Greenbelt, Maryland, USA

Key Points:

- We used the dual AeroCube-6 CubeSats to identify stationary, narrow, and persistent > 30 keV precipitation in low Earth orbit
- 90% of curtains observed are narrower than 21 kilometers in latitude
- A few curtains persistently scattered into the atmosphere for at least six seconds

Corresponding author: M. Shumko, `msshumko@gmail.com`

Abstract

Curtains are recently discovered stationary, persistent, and narrow in latitude electron precipitation phenomena observed in low Earth orbit over sequential passes of the dual AeroCube-6 CubeSats. The > 30 keV electron curtains were stationary over a variety of spacecraft separations, observed by the follower spacecraft up to 65 seconds after the leader. This study expands the recent curtain discovery and quantifies statistical properties of 1634 curtains observed over three years. We found that in low Earth orbit, many curtains are narrower than 10 kilometers in latitude and 90% are less than 21 kilometers wide. We also found that curtains are an outer radiation belt phenomena that are observed in the late morning and midnight magnetic local time, with a higher occurrence rate at midnight. Furthermore curtains are observed more often at lower geomagnetic activity than microbursts. We compare every statistical result to microbursts to test the hypothesis that curtains are drifting remnants of microbursts. Lastly, we found a few curtains in the bounce loss cone region in the north Atlantic Ocean where drift mission is impossible. In one example, a curtain was continuously scattered for at least six seconds so curtains can be a significant source of > 30 keV electrons into the atmosphere.

1 Plain Language Summary

2 Introduction

Curtains are a stationary electron precipitation phenomena observed in low Earth orbit (LEO). They are narrow in latitude, spiky, and appear stationary for up to a minute between subsequent satellite passes. Blake and O'Brien (2016) recently discovered curtains with the > 30 keV electron dosimeters onboard the dual AeroCube-6 (AC6) CubeSats that operated together between 2014 and 2017. This discovery was possible due to AC6's actively maintained in-track separation between a few hundred meters and a few hundred kilometers. Besides the Blake and O'Brien (2016) discovery study not much is known about curtains including what they are, how are they generated, their statistical properties, and their impact on the atmosphere. Answering these questions is an essential next step towards a more complete understanding of how curtains, and particle precipitation in general, affect the magnetosphere and Earth.

Recently developed multi-spacecraft missions, such as AC6, are necessary to identify and distinguish curtains from similar-looking transient precipitation called electron microbursts. Microbursts have been observed since mid 1960s by high altitude balloons and satellites and are also a spiky increase of electrons shorter than a second but are not spatially stationary (e.g. Anderson & Milton, 1964; Lorentzen et al., 2001; O'Brien et al., 2003; Douma et al., 2017). The companion study to this work by Shumko et al. (2019) calculated the spatial size of microbursts using simultaneous observations of microbursts observe by AC6. The impact of microbursts on the environment is substantial. Thorne et al. (2005), Douma et al. (2019), and Breneman et al. (2017)—among others—estimated that microbursts can deplete the outer radiation belt electrons in about a day. Furthermore, Seppälä et al. (2018) modeled a 6 hour microburst storm and concluded that microbursts depleted mesospheric ozone by roughly 10%. Thus, it is important to understand the connection, if any, between microbursts and curtains. Curtains and microbursts can be easily misidentified from a single spacecraft so we need to reevaluate single-satellite microburst studies. If curtains are numerous then the estimated microburst occurrence rates are overestimated. Furthermore, the microburst impact on the atmosphere and the outer radiation belt is also overestimated.

Blake and O'Brien (2016) proposed the following hypothesis that explains curtain-microburst relationship. If a microburst is not completely lost in the atmosphere after the initial scatter, the remaining microburst electrons will spread out (bounce phase average) along the entire magnetic field line. At the same time these electrons drift to the east, with faster energy electrons drifting at a faster rate, so the initially localized mi-

croburst is smeared in longitude into the shape of a curtain. Maybe cite the curtain paper from 2000 that relates them to lightning? Title: Trapped energetic electron curtains produced by thunderstorm driven relativistic runaway electrons.

AC6 does not have the necessary pitch angle, α, resolution to differentiate between drifting and precipitating electrons to test the Blake and O'Brien (2016) hypothesis. Instead we use AC6's position and Earth's asymmetric magnetic field to differentiate particles that are either nearly-trapped or immediately lost in the drift loss cone, and particles immediately lost in the bounce loss cone (BLC). These concepts are described below.

Earth's magnetic field is spatially shifted towards Singapore which creates a region of weaker magnetic field in the South Atlantic Ocean called the South Atlantic Anomaly (SAA). The magnetic field asymmetry caused by the SAA allows barely-trapped particles, defined by a mirror point just above Earth's atmosphere, to mirror much closer to Earth's surface and be lost in the SAA. The barely-trapped particles that are able to execute bounce and drift motion everywhere except the SAA and its conjugate point are in the drift loss cone. The drift loss cone defines a set of α between the trapped and bounce loss cone pitch angles. The particles with pitch angle smaller than the bounce loss cone are unable to complete a full bounce before they are lost in the atmosphere. The convention defining the loss cone is a mirror point at or below 100 kilometer altitude. In this study we will use this definition as well as a more strict convention of a mirror point below sea level.

Without pitch angle resolution, we use AC6's location in LEO to isolate particles that are trapped, barely-trapped, and immediately lost. Above the SAA, AC6 will observe, but not differentiate, particles that are trapped, barely-trapped, and immediately precipitating. In the region outside of the SAA and it's conjugate point, AC6 will observe particles barely trapped in the drift loss cone and immediately precipitating in the bounce loss cone. Lastly, the region in the North Atlantic that is magnetically conjugate to the SAA is the bounce loss cone. Here AC6 only observes particles precipitating within a bounce period ($\approx$ 1.5 second for 30 keV electrons). If a particle makes it to AC6's altitude, it can gyrate past AC6 and precipitate in the North Atlantic. Alternatively, the particle will mirror at or below AC6 and gyrate into the SAA where the equivalent mirror point magnetic field strength is deep in the atmosphere, or below sea level. Thus the particle is lost. Therefore, any precipitation structures observed in the bounce loss cone region must rapidly precipitate.

Think about how Max Comess explained the BLC. Am I going overboard?... The bounce loss region is defined as where the field of view of the PET and HILT detectors are fully within the bounce loss cone, where the bounce loss cone is defined such that any electrons detected should precipitate on their next bounce, ensuring that any particles viewed by SAMPEX in this region are not trapped, nor were they scattered into the loss cone at a substantially different MLT than SAMPEXs location. These criteria put SAMPEX in the north Atlantic (Figure 1), conjugate to the outer-belt portion of the South Atlantic Anomaly [see, e.g., Dietrich et al., 2010, Figure 3].

This study expands the Blake and O'Brien (2016) study by estimating statistical properties of curtains and address the Blake and O'Brien (2016) hypothesis. We use 1634 confirmed curtain observations to learn about the distributions of: the curtain width in latitude, the geomagnetic conditions favorable to curtains, and curtain distribution in L and magnetic local time (MLT). Lastly we will address the hypothesis that curtains are drifting remnants of microbursts by showing examples of curtains observed in the bounce loss cone region.

3 Instrumentation

The AC6 mission was a pair of 0.5U (10x10x5 cm) CubeSats built by The Aerospace Corporation designed to measure the electron and proton environment in low Earth orbit (O'Brien et al., 2016). AC6 was launched on 19 June 2014 into a 620x700 km, 98° inclination orbit. The AC6 orbit over the three year mission lifetime was roughly dawn-dusk, and precessed only a few hours in MLT; 8-12 MLT in dawn and 20-24 MLT in dusk. The two AC6 spacecraft, designated as AC6-A and AC6-B, separated after launch and were in proximity for the duration of the three year mission—maintained by an active attitude control system. The attitude control system allowed then to precisely control the amount of atmospheric drag experienced by each AC6 unit using the surface area of their solar panel "wings". By changing their orientation, AC6 was able to maintain a separation between 2-800 km, confirmed with the Global Positioning System. The two AC6 units were in a string of pearls configuration so one unit, typically unit A, was leading the other by an in-track lag—the time it would take the following spacecraft to catch up to the position of the leading spacecraft. To convert between the AC6 in-track separation and in-track lag, we assume a typical 7.5 km/s orbital velocity of LEO spacecraft. The in-track lag was readily available with the Global Positioning System which makes it easy to study precipitation phenomena observed at the same time, and at the same position by shifting one time series by the in-track lag.

Each AC6 unit contains three Aerospace microdosimeters (licensed to Teledyne Microelectronics, Inc) that measure the electron and proton dose in orbit (O'Brien et al., 2016). The dosimeter used for this study is dos1 with a 30 keV electron threshold. dos1 is used for this study because the other dosimeters were not identical between unit A and B. All dosimeters sample at 1 Hz in survey mode, and 10 Hz in burst mode. 10 Hz data was readily available from both AC6 units from June 2014 to May 2017 while their in-track lag was less than 65 seconds, and at times was a fraction of a second. Show a distribution of the in-track lag when they had 10 Hz data? The variety of AC6 separations and data availability over the three-year mission makes it possible to study tranisent electron microburst precipitation (Shumko et al., 2019) and now stationary electron curtain precipitation.

4 Methodology

4.1 Curtain Identification

Outline

1. Mention that various parameters were explored and we tuned it to have as many candidate events as possible while being feasible to inspect every detection.

The 10 Hz data was used to identify curtains with the following two criteria: a high spatial correlation, and spiky. The first criterion quantifies the similarity of the feature between both AC6 units, and the second criterion checks that highly correlated times were spiky. Before we we applied the identification criteria, the AC6-B time series was shifted by the in-track lag to spatially align it with the AC6-A time series.

The first identification criterion is a 1-second rolling Pearson correlation applied to both time series. Spatial features with a correlation greater than 0.8 were considered highly correlated and saved.

The second identification criterion checks for locations where both AC6 units observed spiky precipitation. Similar to how precipitation bands were identified in Blum et al. (2015) and microbursts in Greeley et al. (2019), we find spiky precipitation by estimating the number of Poisson standard deviations, σ, that a dos1 count rate is above

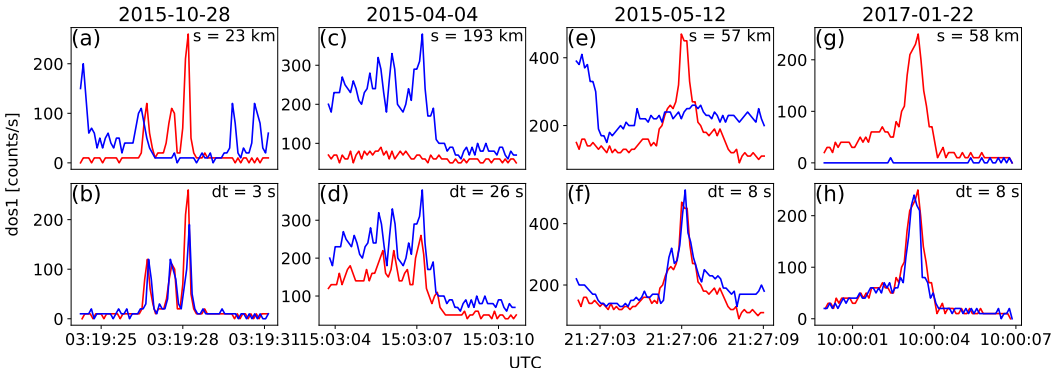

Figure 1. Four examples showing the AC6 > 30 keV electron data taken by AC6 at the same time in the top row and at the same position in the bottom row. AC6-A, whose data is shown with red curves, was s kilometers ahead of AC6-B. To show the data at the same position the time series data from one spacecraft was shifted by the in-track lag and annotated by dt. These examples show curtain precipitation that was highly correlated for up to 26 seconds.

a centered 10-second running average, B_{10}. Locations where the count rates are at least two σ above B_{10} are spiky.

The locations where the two criteria are met are curtain candidates and the time of the peak count rates are saved. To check the quality of the data set, one author visually checked every candidate curtain and 1634 curtains were confirmed. Four curtain examples are shown in Fig. 1. In these examples the unmodified time series is in the top row and the corresponding spatially-aligned time series is in the bottom row. The in-track lag used to shift the bottom row is annotated by dt, corresponding to an AC6 in-track separation annotated by s. The top row is uncorrelated; thus these events were not microbursts. The bottom row is correlated after 3 to 26 seconds. The correlated curtains in the bottom row are peculiar—they have a fine structure on a 10-kilometer scale that we have shown to persist for at least 26 seconds.

5 Results

In the spirit of brevity, we limited the scope of this statistical study to answer three questions:

1. How narrow are curtains?
2. When and where are curtains observed?
3. Are curtains drifting or locally precipitating?

For each of these questions we will compare the curtain distribution with the > 30 keV microburst distribution from Shumko et al. (2019). Lastly, we will show evidence that suggests that some curtains are continuously scattered and not drifting.

5.1 Curtain Width

We quantified curtain width in time as the width at half of the curtain's topographic prominence: the height of the peak above the lowest contour that encircles the peak but contains no higher peak. The spatial width of a curtain is the product of the temporal width and the 7.5 km/s orbital velocity mostly in latitude. The distribution of curtain

widths is shown in Fig. 2 by the thick black curve. Curtains are very narrow in latitude. Many curtains are less than 10 km wide, and 90% are narrower than 21 km.

We compared the curtain width distribution to the microburst size distribution estimated in Shumko et al. (2019). Shumko et al. (2019) estimated the microburst size distribution by finding microbursts that were observed simultaneously by both AC6 units so the microburst size much be larger than the AC6 separation. The red curve in Fig. 2 shows the microburst distribution estimated from the ratio of the number of concurrent and nonconcurrent microbursts observed in each separation bin.

The curtain and microburst size distributions are very similar with a one notable difference. Curtain widths are observed directly hence their distribution is peaked, while the microburst distribution is estimated from concurrent observations so their distribution is peaked at 0 km AC6 separation.

5.2 When and Where Are Curtains Observed

The distribution of curtains in L and MLT is shown in Fig. 3. Figure 3a shows the distribution of the 1634 observed curtains and Fig. 3b shows the normalized distribution. The white bins, mostly in the early morning and evening MLT regions, had no observed curtains because the AC6 orbit did not sample there. Figure 3c confirms this by showing the distribution of the number of quality (data quality flag = 0) 10 Hz samples.

After scaling by the uneven sampling in the late morning and midnight MLT regions, the normalized distribution in Fig. 3b shows enhanced curtain occurrence in the outer radiation belt in late morning and midnight MLT regions.

Now we quantify the geomagnetic conditions favorable for curtains. Figure 4 shows the distribution of the Auroral Electroject (AE) index between 2014 and 2017, and the distribution of the AE index when curtains and microbursts were observed. The distribution of the AE index when > 30 keV microbursts were observed is shown with a dashed green curve. Curtains are observed typically when AE is enhanced. Microbursts are observed when AE is enhanced more than for curtains.

5.3 Local Atmospheric Precipitation

Now we will show examples of curtains that were scattered over an extended period of time in the bounce loss cone. We estimated the bounce loss cone region in the North Atlantic Ocean using the IRBEM-Lib magnetic field library (Boscher et al., 2012). First we estimated the local magnetic field strength on a latitude-longitude grid spanning the North Atlantic, at 700 kilometer altitude that is typical for AC6. For each latitude-longitude point we traced that magnetic field line to the SAA and found the position along that field line with an equivalent field strength as in the North Atlantic. A particle that mirrors at the grid location will mirror and gyrate to the southern hemisphere before mirroring at an altitude with the eqivulant field strength or be lost in the atmosphere. Since we are considering particles mirroring at the grid points in North Atlantic, this estimate is the upper bound altitude that the particle can mirror. Particles mirroring above the grid will not be observed, and the particles that are observed will mirror at or below the estimated altitude in the SAA. If the corresponding field strength position is at 100 kilometers or lower in the SAA we considered that grid point in the North Atlantic in the bounce loss cone region. For the more rigorous bounce loss cone criteria, we saved the grid locations where the equivalent field strength altitude in the SAA is below sea level.

Figure 5a shows a map of the bounce loss cone region in the North Atlantic. The solid blue line is the north bound of the region where a particle observed at 700 kilometers at that location will mirror at 100 kilometers in the SAA. Immediately south of the solid blue line the SAA mirror altitude rapidly decreases towards, and below, sea level.

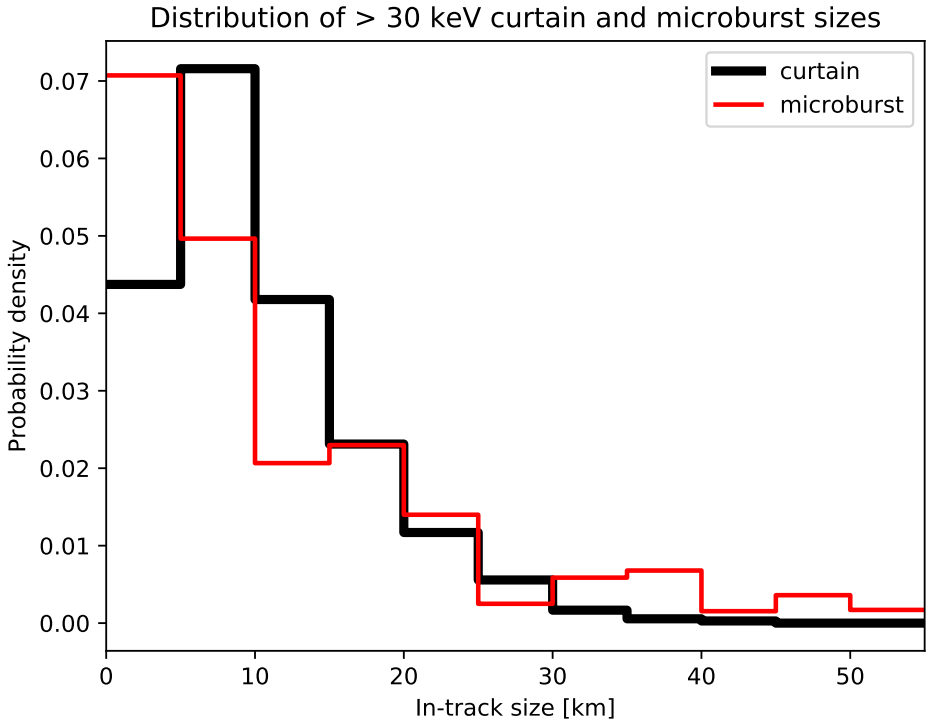

Figure 2. Size distributions of curtains (AC6 in-track separation mostly in latitude) in black and microbursts in red as a function of AC6 in-track width. Microburst distribution adopted from Shumko et al. (2019).

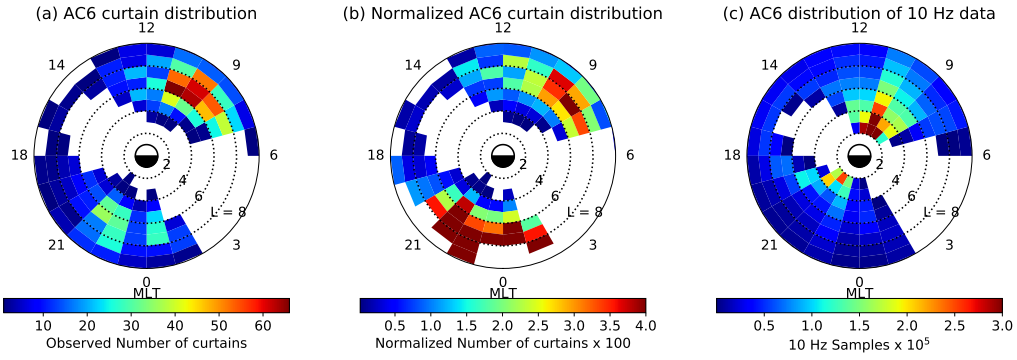

Figure 3. Distribution of observed curtains as a function of L and MLT in panel a and normalized number of curtains in panel b. Panel c shows the number of quality 10 Hz samples taken at the same time that was used to normalize panel b. The white bins in panels a have 0 curtain observations. In panel b the white shaded bins had either 0 detections or very little 10 Hz samples (less than $10,000$).

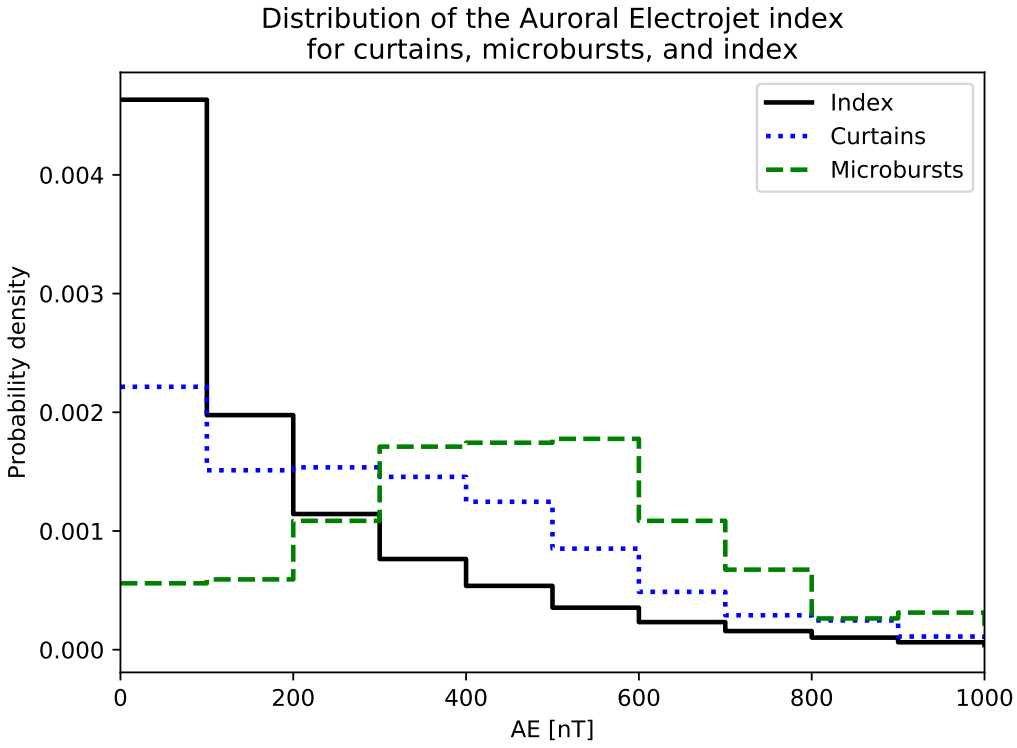

Figure 4. The distribution of the Auroral Electroject (AE) index from 2014 to 2017. The black curve shows the distribution for the entire 2014-2017 AE data set, the dotted blue curve shows the AE distribution for curtains, and the dashed green curve shows AE the distribution for microbursts studied in Shumko et al. (2019).

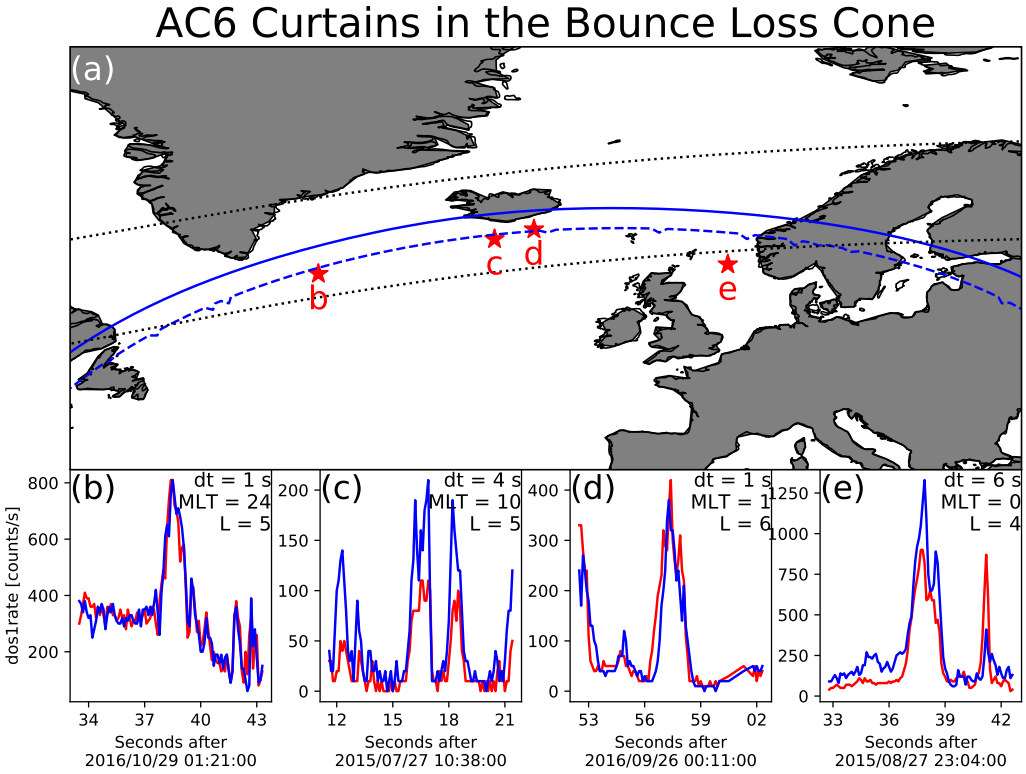

Figure 5. Curtains observed inside the bounce loss cone region. Panel a shows a map of the North Atlantic region with the outer radiation belt, defined by an L shell range between 4 and 8, shown with the dotted black curves. The solid blue curve shows the northern boundary of the bounce loss cone region. Along this curve, electrons observed at a 700 kilometer altitude in the North Atlantic will mirror at 100 kilometers in the SAA. A more strict bounce loss cone criteria is the dashed blue curve that represents a mirror point altitude at sea level in the SAA. The 4 red stars with labels show the locations of the curtain examples shown in panels b-e. The panels b-e show the 4 example curtains with the AC6-A shown by the red line, and AC6-B with the blue line. AC6-A was ahead in all examples except panel d.

The dashed blue line is the set of latitude-longitude points where the SAA mirror point altitude is at sea level. Furthermore we superposed two dotted black lines on Fig. 5a that represent the boundary of the outer radiation belt defined between L shells of 4 and 8. The bounce loss cone region here closely matches the region shown in Comess et al. (2013, Figure 1) and Dietrich et al. (2010, Figure 3). We used the Olson-Pfitzer magnetic field model (Olson & Pfitzer, 1982) to estimate the bounce loss cone boundary. The same analysis using the Tsyganenko 1989 model (Tsyganenko, 1989) yielded similar boundaries.

We found four good curtains that were observed inside the bounce loss cone regions and included the shifted time series plots in Fig. 5b-e, with the AC6 in-track lag, L and MLT of the observations annotated. The AC6 locations where these curtains were observed are shown in 5a with red stars and the corresponding panel labels. The curtains shown in Fig. 5c and e were observed near the sea level SAA mirror altitude curve thus they were not drifting and were precipitating as much as 6 seconds as shown in Fig. 5e. For reference, the precipitation persisted for longer than the typical ≈ 1.5 second bounce period of 30 keV electrons in this region.

6 Discussion

Outline

1. AC6 can't answer this question, but curtains could provide a substantial source of HOx and NOX molecules responsible for destroying ozone. We need AC6 with energy and pitch angle resolution.

6.1 Curtain Width In Latitude

Curtains are very narrow in latitude. Figure 2 shows the width in latitude of many curtains are on the order of 10 kilometers and 90% are narrower than 21 km. Scaled to the magnetic equator, where we presume curtains are generated, these latitudinal widths correspond to a source with a radial scale size of a few hundred kilometers. As shown in Fig. 1f and 1h; it is remarkable that some curtains maintain a fine structure after multiple seconds with little observable difference. Sometimes curtains appear to be slightly and systematically shifted in latitude, while maintaining their shape (not shown).

If curtains are remnants of microbursts then the distribution of curtain widths in latitude correspond to the microburst size distribution. Figure 2 shows a good correspondence between the distribution of curtain widths in latitude and the microburst size distribution from Shumko et al. (2019). Therefore, it is reasonable to believe that curtains and microbursts are related, but this result need to be closely inspected for sources of bias.

The microburst scale size distribution, as described in Shumko et al. (2019), is the fraction of microbursts observed simultaneously to all microbursts observed either simultaneously or by only one AC6 unit. A microburst observed simultaneously must be larger than the spacecraft separation so the microburst distribution represents a lower bound. Shumko et al. (2019) attempted to account for this bias but it is difficult. This bias that shifts the microburst distribution to smaller sizes so in the microburst size distribution shown in Fig. 2 is underestimated.

Furthermore the detection algorithm described in section 4.1 has a width bias. For wide curtains with a similar width to the detection algorithm's 10-second baseline, the 10-second baseline is then calculated using the enhanced curtain counts instead of the background and is increased above the true background and thus the curtain peak is less pronounced relative to the baseline. As a result, the curtain detection algorithm is less sensitive to wider curtains. The result of this bias is similar to the bias inherent in the microburst distribution—the curtain widths are underestimated.

Both of these biases underestimate the true size of curtains and microbursts, so this evidence agrees with the Blake and O'Brien (2016) microburst-curtain hypothesis.

6.2 When and Where Are Curtains Observed

Figure 3 shows that curtain phenomena originates in the outer radiation belt, and observed relatively more in the evening than morning regions. Unfortunately, the limited AC6 coverage prevents a complete curtain distribution in MLT. From the MLT information we have in Fig. 3b, curtains are most often observed near midnight MLT with relatively less observed in the late morning MLT. This distribution, though limited, appears to be similar to the L-MLT distribution of microbursts from prior studies (e.g. O'Brien et al., 2003; Douma et al., 2017).

Curtains also exhibit a preference to disturbed geomagnetic conditions as shown in Fig. 4, but not as disturbed as microbursts from Shumko et al. (2019). A possible explanation: during quiet conditions the remnant microburst electrons are more likely to

drift undisturbed and AC6 is more likely to observe the fine, highly-correlated curtain structure. In contrast, during active conditions curtain electrons are still drifting, but the dynamics of an actively-changing magnetosphere can easily perturb curtain electrons until AC6 no longer observes a highly correlated structure at the same location.

6.3 Curtains Observed in The Bounce Loss Cone

Lastly we address curtains observed in the bounce loss cone. What can cause continuous, $>$ 30 keV electron precipitation observed for multiple seconds? The precipitation mechanism responsible must be radially localized near the magnetic equator, on a scale of a few hundred kilometers. One potential driver is a parallel DC electric field that lowers the mirror point to AC6 altitudes. We now estimate the minimum potential that can accelerate these curtain electrons and lower the mirror point. We assume the particle is initially just trapped with a mirror point at 100 kilometers in the SAA. This condition implies that the particle's mirror point in the bounce loss cone is above AC6.

To find the parallel potential potential we use the kinetic energy, W, of a 30 keV particle at its initial mirror point at a magnetic field strength of B_i. The kinetic energy can be written as $W_i = \mu B_i$ where $\mu \sim W_\perp/B$ is the first adiabatic invariant, and $W_\perp$ is the kinetic energy of the particle perpendicular to the background magnetic field. Now when a parallel potential acts on the electron of charge q and does $q\Phi$ amount of work, the electron will mirror closer to Earth's surface and mirror at a field strength B_f where its final energy is $W_f = \mu B_f$. Now we relate the initial and final states of the electron,

$$\mu B_f = \mu B_i + q\Phi \tag{1}$$

which can be rewritten as Check if this jump is easy to follow

$$q\Phi = W\frac{(B_f - B_i)}{B_i}. \tag{2}$$

We again use IRBEM-Lib to estimate $q\Phi$. For each example curtain in Fig. 5, we traced the field line from AC6 into the SAA. Then we found B_i at 100 kilometers altitude in the SAA for barely trapped electrons. With the local magnetic field strength at AC6 as B_f, we estimated the minimum potential necessary to lower a 30 keV particle's mirror point to be 1-4 kV. Recalculate these potentials for the four cases. Also cite FAST paper here.

7 Conclusions

Acknowledgments

This work was made possible with the help from the many engineers and scientists at The Aerospace Corporation who designed, built, and operated AC6. M. Shumko was supported by NASA Headquarters under the NASA Earth and Space Science Fellowship Program - Grant 80NSSC18K1204. D.L. Turner is thankful for support from the Van Allen Probes mission and a NASA grant (Prime award number: 80NSSC19K0280). The work at The Aerospace Corporation was supported in part by RBSP-ECT funding provided by JHU/APL contract 967399 under NASA's Prime contract NAS501072. The AC6 data is available at http://rbspgway.jhuapl.edu/ac6 and the IRBEM-Lib version used for this analysis can be downloaded from https://sourceforge.net/p/irbem/code/616/tree/.

8 Homeless Words

Title: Statistical Properties of Curtains–Latitudinally-Narrow and Persistent Electron Precipitation Phenomena

This study leverages AC6, a multi-spacecraft mission, to interpret and understand particle precipitation in a way that is impossible with a single spacecraft.

This study leverages the asymmetry in Earth's magnetic field. The asymmetric magnetic field results in the SAA and the BLC, two very related and unique regions

Particles that impact the atmosphere are lost during that bounce motion. We found curtains in the bounce loss cone, a region in the North Atlantic near and above Iceland.

The bounce loss cone is magnetically connected to the SAA, where Earth's magnetic field is weakest near Earth's surface. A particle observed in the blc in the northern hemisphere will descend below 100 km altitude. At sub-100 km altitudes the particle has a high chance of encountering and scattering with the atmosphere and be lost.

We found curtain electrons that, when given the chance to execute their cyclical bounce motion, will descend below Earth's surface in the SAA. An electrons can not survive that trip.

Write the paper and ask the question: "What is this paper really about?" Not just curtains, but uncovering something unexpected that has been observed and overlooked for decades.

Are curtains related to aurora? This is a good question—one that is not pertinent here (idea from The Elements of Style p.68).

Here are two parting questions that are not considered here. Why were some curtains shifted slightly? Perhaps it was due to the movement of the magnetic field lines. Also do curtains have a corresponding visual signature on the ground? The answer to this question will show if curtains are related to the aurora.

References

Anderson, K. A., & Milton, D. W. (1964). Balloon observations of X rays in the auroral zone: 3. High time resolution studies. *Journal of Geophysical Research*, *69*(21), 4457–4479. Retrieved from `http://dx.doi.org/10.1029/JZ069i021p04457` doi: 10.1029/JZ069i021p04457

Blake, J. B., & O'Brien, T. P. (2016). Observations of small-scale latitudinal structure in energetic electron precipitation. *Journal of Geophysical Research: Space Physics*, *121*(4), 3031–3035. Retrieved from `http://dx.doi.org/10.1002/2015JA021815` (2015JA021815) doi: 10.1002/2015JA021815

Blum, L., Li, X., & Denton, M. (2015). Rapid MeV electron precipitation as observed by SAMPEX/HILT during high-speed stream-driven storms. *Journal of Geophysical Research: Space Physics*, *120*(5), 3783–3794. Retrieved from `http://dx.doi.org/10.1002/2014JA020633` (2014JA020633) doi: 10.1002/2014JA020633

Boscher, D., Bourdarie, S., O'Brien, P., Guild, T., & Shumko, M. (2012). *Irbem-lib library.*

Breneman, A., Crew, A., Sample, J., Klumpar, D., Johnson, A., Agapitov, O., ... others (2017). Observations directly linking relativistic electron microbursts to whistler mode chorus: Van allen probes and FIREBIRD II. *Geophysical Research Letters*.

Comess, M., Smith, D., Selesnick, R., Millan, R., & Sample, J. (2013). Duskside relativistic electron precipitation as measured by sampex: A statistical sur-

vey. *Journal of Geophysical Research: Space Physics*, *118*(8), 5050-5058. Retrieved from https://agupubs.onlinelibrary.wiley.com/doi/abs/10.1002/jgra.50481 doi: 10.1002/jgra.50481

Dietrich, S., Rodger, C. J., Clilverd, M. A., Bortnik, J., & Raita, T. (2010). Relativistic microburst storm characteristics: Combined satellite and ground-based observations. *Journal of Geophysical Research: Space Physics*, *115*(A12).

Douma, E., Rodger, C., Blum, L., O'Brien, T., Clilverd, M., & Blake, J. (2019). Characteristics of relativistic microburst intensity from sampex observations. *Journal of Geophysical Research: Space Physics*.

Douma, E., Rodger, C. J., Blum, L. W., & Clilverd, M. A. (2017). Occurrence characteristics of relativistic electron microbursts from SAMPEX observations. *Journal of Geophysical Research: Space Physics*, *122*(8), 8096–8107. Retrieved from http://dx.doi.org/10.1002/2017JA024067 (2017JA024067) doi: 10.1002/2017JA024067

Greeley, A., Kanekal, S., Baker, D., Klecker, B., & Schiller, Q. (2019). Quantifying the contribution of microbursts to global electron loss in the radiation belts. *Journal of Geophysical Research: Space Physics*.

Lorentzen, K. R., Blake, J. B., Inan, U. S., & Bortnik, J. (2001). Observations of relativistic electron microbursts in association with VLF chorus. *Journal of Geophysical Research: Space Physics*, *106*(A4), 6017–6027. Retrieved from http://dx.doi.org/10.1029/2000JA003018 doi: 10.1029/2000JA003018

O'Brien, T. P., Blake, J. B., & W., G. J. (2016, May). *Aerocube-6 dosimeter data readme* (Tech. Rep. No. TOR-2016-01155). The Aerospace Corporation.

O'Brien, T. P., Lorentzen, K. R., Mann, I. R., Meredith, N. P., Blake, J. B., Fennell, J. F., ... Anderson, R. R. (2003). Energization of relativistic electrons in the presence of ULF power and MeV microbursts: Evidence for dual ULF and VLF acceleration. *Journal of Geophysical Research: Space Physics*, *108*(A8). Retrieved from http://dx.doi.org/10.1029/2002JA009784 doi: 10.1029/2002JA009784

Olson, W. P., & Pfitzer, K. A. (1982). A dynamic model of the magnetospheric magnetic and electric fields for july 29, 1977. *Journal of Geophysical Research: Space Physics*, *87*(A8), 5943–5948. Retrieved from http://dx.doi.org/10.1029/JA087iA08p05943 doi: 10.1029/JA087iA08p05943

Seppälä, A., Douma, E., Rodger, C., Verronen, P., Clilverd, M. A., & Bortnik, J. (2018). Relativistic electron microburst events: Modeling the atmospheric impact. *Geophysical Research Letters*, *45*(2), 1141–1147.

Shumko, M., Johnson, A., Sample, J., Griffith, B. A., Turner, D. L., O'Brien, T. P., ... Claudepierre, S. G. (2019). Electron microburst size distribution derived with aerocube-6. *Journal of Geophysical Research: Space Physics*, e2019JA027651.

Thorne, R. M., O'Brien, T. P., Shprits, Y. Y., Summers, D., & Horne, R. B. (2005). Timescale for MeV electron microburst loss during geomagnetic storms. *Journal of Geophysical Research: Space Physics*, *110*(A9). Retrieved from http://dx.doi.org/10.1029/2004JA010882 (A09202) doi: 10.1029/2004JA010882

Tsyganenko, N. (1989). A solution of the chapman-ferraro problem for an ellipsoidal magnetopause. *Planetary and Space Science*, *37*(9), 1037 - 1046. Retrieved from http://www.sciencedirect.com/science/article/pii/0032063389900767 doi: http://dx.doi.org/10.1016/0032-0633(89)90076-7